Materials and Design 109 (2016) 153–161

Contents lists available at ScienceDirect

Materials and Design

journal homepage: www.elsevier.com/locate/matdes

Nanosecond pulsed laser irradiation induced hierarchical micro/nanostructures on Zr-based metallic glass substrate

Hu Huang [a], Noguchi Jun [a], Minqiang Jiang [b], Moriya Ryoko [a], Jiwang Yan [a,*]

[a] Department of Mechanical Engineering, Faculty of Science and Technology, Keio University, Yokohama 223-8522, Japan
[b] State Key Laboratory of Nonlinear Mechanics, Institute of Mechanics, Chinese Academy of Sciences, Beijing 100190, People's Republic of China

HIGHLIGHTS

- Hierarchical micro/nanostructures were fabricated on a metallic glass substrate by nanosecond pulsed laser irradiation.
- It retained amorphous characteristic and exhibited uniform element distribution.
- Irradiation parameters induced change from cotton-like to particle-like nanostructure.
- Formation mechanism and mechanical properties were investigated.

GRAPHICAL ABSTRACT

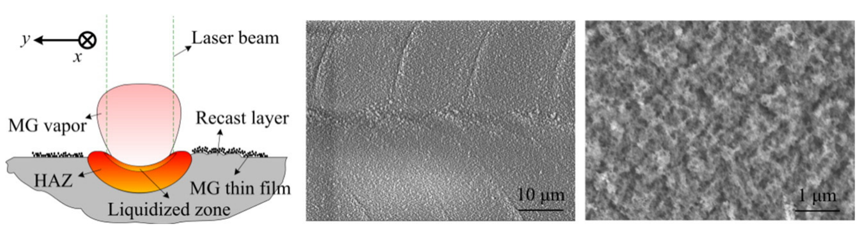

ARTICLE INFO

Article history:
Received 19 March 2016
Received in revised form 17 June 2016
Accepted 12 July 2016
Available online 14 July 2016

Keywords:
Hierarchical micro/nanostructure
Metallic glass
Thin film
Laser irradiation
Nanoindentation

ABSTRACT

A large effective surface area is beneficial to enhance the applications of metallic glasses (MGs) in heterogeneous catalysis and biomedical engineering. For the purpose of increasing effective surface area, in this study, hierarchical micro/nanostructures were fabricated on a Zr-based MG substrate by nanosecond pulsed laser irradiation. Experimental results indicated that a layer of micron-scale laser pulse tracks covered by a cotton-like MG thin film with nanometer-scale microstructure was formed in the laser irradiated region. This hierarchical micro/nanostructures retained amorphous characteristic and exhibited uniform element distribution. Its formation mechanism was investigated by analyzing the laser irradiation process and morphologies. Nanoindentation results indicated that the cotton-like MG thin film was very loose and soft compared to the as-cast MG substrate, showing different plastic deformation behavior. Results from this study indicate that nanosecond pulsed laser irradiation is an effective method to generate hierarchical micro/nanostructures on MG substrates, which can increase their effective surface areas and improve their potential applications as biomaterials and catalysts.

1. Introduction

Due to absence of dislocations and grain boundaries which are typically observed in crystalline materials, metallic glasses (MGs) without long-range topological order show excellent mechanical and chemical properties, such as high hardness and strength, large elastic limit as well as superior resistance to wear and corrosion [1–4]. These features make MGs to be regarded as very promising structural, engineering, and sport materials [5,6]. Furthermore, MGs also show potentials in heterogeneous catalysis and biomedical engineering, but the featureless structure of the as-cast MGs significantly reduces their applicability in these fields because of small effective surface areas [7]. To solve this problem, introducing micro/nanostructures with enhanced effective surface areas into MGs is of great importance [7–9]. For example, via magnetron sputtering using mixed powders, Chen et al. [7] prepared a gold-based MG showing a heterogeneously granular structure with nanoparticles, which exhibited a high catalytic activity in the oxidation of organosilane compounds with water. By the same method, Zr–Pd MG thin films with a similar nanometer-scale surface structure were

* Corresponding author.
E-mail address: yan@mech.keio.ac.jp (J. Yan).

http://dx.doi.org/10.1016/j.matdes.2016.07.056
0264-1275/

prepared by the same research group [8], which showed good biocompatibility for potential applications in biochemistry and implant engineering. Zhao et al. [9] used a chemical method to fabricate MG nanoparticles, which showed applications as highly durable catalysts in methanol electro-oxidation. However, these methods may be only suitable to certain kinds of MGs, and furthermore they are not economical or environmental-friendly [10,11]. Hence, new methods to generate micro/nanostructures on MG surfaces are greatly desired for their wide applications.

Although mechanical machining, typically diamond cutting [12–14], has been widely used to fabricate micro/nanostructures on the surface of soft metals because of its flexibility, such as copper by tuning tool paths [15], it may be not suitable for MGs. The high hardness of MGs (usually 6–8 times of copper) accelerates the tool wear which affects the uniformity and accuracy of the cutting surface [16,17]. For some hard-brittle MGs, mechanical machining becomes more difficult. For example, most of Fe-based MGs show high hardness (~12 GPa) but very low fracture toughness (~10 MPa $m^{1/2}$) [18], although some Fe-based MGs with enhanced ductility had been reported recently [19]. Furthermore, very low thermal conductivity of MGs results in a high local temperature in the cutting region especially during high speed cutting. Thus, oxidation and crystallization of MGs may occur [20] which probably affect their amorphous performances [21,22], but this kind of effects is dependent of the properties and volume fraction of the crystalline phases [21–23] as well as the sample preparation and evaluation methods [24,25]. In addition, high local temperature will also increase the adhesion between the chip and tool, leading to the formation of built-up edge on the rake face, and thus affect the subsequent cutting process [16,26]. Hence, fabrication of micro/nanostructured surfaces on MGs by mechanical machining is challenging.

Taking the feature of viscous state in the supercooled temperature region (between the glass transition and crystallization temperature), thermoplastic shaping was reported to form micro/nanostructured surfaces on MGs [27–29]. However, the high cost to fabricate the micro/nanostructured molds as well as the limited mold-life-times hinders its wide applications [2]. Furthermore, crystallization may also occur during the thermoplastic shaping because it is very hard to control a uniform forming temperature [30], especially for MGs with a narrow supercooled temperature region.

In recent years, nanosecond pulsed laser irradiation was adopted to fabricate micro/nanostructured surfaces that possess unique optical, photoelectric, catalytic, mechanical, and wetting properties. For example, superhydrophobic surfaces were obtained by nanosecond laser texturing or ablation [31]. Via nanosecond laser ablation, micro/nanostructures were patterned on silicon surface [32], resulting in decreased reflectivity, which has potential applications in solar cells. For MGs, previous studies by nanosecond pulsed laser irradiation with a single shot showed that surface ripple patterns as well as porous structure consisting of 100 nm-scale voids were formed in the irradiated area [33–35]. However, large-area nanosecond pulsed laser irradiation of MG surfaces has been rarely investigated, but it has the potential to generate hierarchical micro/nanostructured surfaces with enhanced effective surface areas according to the following considerations. Firstly, during single pulsed laser shot, a micro-crater can be formed. If line irradiation is implemented along two directions with an overlapped region between two craters, a layer of laser pulse tracks can be patterned on MGs. Secondly, when the laser intensity is sufficiently high, the irradiated materials may experience phase changes, vaporization, boiling, and even explosive boiling, accompanying with the ejection of a high-temperature matter because of the recoil pressure [34–38]. By re-deposition of the vapor particles in the adjacent irradiated region, a layer of MG thin film is expected to be formed over the first layer of laser pulse tracks. According to aforementioned analysis, we attempt to fabricate hierarchical micro/nanostructured surfaces on a MG substrate via nanosecond pulsed laser irradiation in this study, and further discuss its formation mechanism as well as mechanical properties.

2. Experimental procedure

$Zr_{41.2}Ti_{13.8}Cu_{12.5}Ni_{10}Be_{22.5}$ MG sample (commonly called Vitreloy 1 [39]) with a diameter of 10 mm and thickness of 2 mm was used. Before laser irradiation, it was mechanically polished using 400, 800, and 1500 grit sand papers in sequence. A Nd:YAG nanosecond pulsed laser system (LR-SHG, MegaOpto Co., Ltd., Japan) with a wavelength of 532 nm and a pulse width of 15.4 ns was used. The laser beam was shaped to a square section of ~85 μm × 85 μm. The pulse frequency was kept 1 kHz, and the overlapped region between two scanning lines was 45 μm. Various scanning speeds, 1, 5, and 10 mm/s, were used during laser irradiation, which theoretically resulted in various overlapped regions along a scanning line, 84, 80, and 75 μm, respectively. Also various average laser powers (0.013–0.649 W) were used, corresponding to peak laser powers in the range of 8.4×10^2–4.2×10^4 W. According to Ref. [40], the peak laser power intensity was calculated to be in the range of 1.2×10^{11}–5.8×10^{12} W/m^2. To avoid oxidation, vacuum environment was realized by 5 min vacuum pumping of the sample chamber (65 mm × 65 mm × 45 mm) before laser irradiation.

Microstructures of the MG after laser irradiation were observed by a three dimensional (3D) laser scanning microscope (VK-9700, Keyence, Japan) and a field emission scanning electron microscope (FE-SEM) (JSM-7600F, JEOL, Japan). An X-ray diffractometer (XRD, D8 Discover, Bruker, Germany) was used to characterize the amorphous characteristic of the MG before and after laser irradiation. Element mapping was performed on the irradiated region by an energy dispersive X-ray spectroscopy (EDX, XFlash Detector 4010, Bruker, Germany). Nanoindentation tests were performed on an ENT-1100 nanoindentation instrument (Elionix Inc., Japan) equipped with a Berkovich type diamond indenter, and their residual morphologies were also observed by the FE-SEM.

3. Results and discussion

3.1. Morphological analysis

Fig. 1 presents representative optical morphologies of the laser irradiated region under an average power of 0.402 W and scanning speed of 10 mm/s. Under this condition, the peak laser power and power intensity was 2.6×10^4 W and 3.6×10^{12} W/m^2, respectively, and the laser fluence was 5.6 J/cm^2. In Fig. 1(a), a rectangle irradiated region was formed on the MG surface. Laser irradiation started from the upper-right corner and ended at the bottom-right corner. Fig. 1(b) gives the local enlarged view of Fig. 1(a), where many remarkable laser pulse tracks are observed. The reversed direction between two adjacent scanning lines results from reversed laser scanning direction. Fig. 1(c) shows the 3D morphology corresponding to Fig. 1(b), and Fig. 1(d) and (e) show the profiles along the solid line and dashed line in Fig. 1(b), respectively. The height of laser pulse tracks periodically varies in micron-scale in both x and y directions. The curved surface can effectively increase the surface area. For example, the measurement result by the 3D laser scanning microscope indicates that the effective surface area for the evaluated region in Fig. 1(c) is 1.57 times of the corresponding flat surface area. From Fig. 1, it can be concluded that a layer of laser pulse tracks in micron-scale has been successfully formed in the irradiated region. It should be noted that the microstructure and height shown in Fig. 1 can be tuned easily by changing the laser scanning speed, power and overlapped region, resulting in various effective surface areas.

Because the optical microscope had a limited magnification, FE-SEM was used to further observe the detailed microstructure in the irradiated region shown in Fig. 1 with higher magnifications, and results are presented in Fig. 2. In Fig. 2(a), the irradiated region (region 1) is surrounded by a grey region (region 2) with a width of ~370 μm, which is the heat affected zone (HAZ). Fig. 2(b), (c), and (d) are the local enlarged views of the region 1, and Fig. 2(e) and (f) are the local